The Strength and Fracture Toughness of 18 Ni (350) Maraging Steel

H. J. RACK AND DAVID KALISH

The influence of microstructure on the strength and fracture toughness of 18 Ni (350) maraging steel was examined. Changes in microstructure were followed by X-ray and neutron diffraction and by optical and electron microscopy. These observations have been correlated with the fracture morphology established by scanning electron microscopy. Air cooling this alloy from the austenitizing temperature results in a dislocated martensite. During the initial stage of age hardening, molybdenum atoms tend to cluster (forming preprecipitates) and the cobalt assumes short range ordered positions. Subsequent aging results in Ni_3Mo and σ-FeTi with overaging being associated with the formation of equilibrium reverted austenite and Fe_2Mo. The fracture behavior is examined in terms of elementary dislocation precipitate interactions. It is suggested that the development of coplanar slip in the underaged conditions leads to its increased stress corrosion susceptibility and decreased fracture toughness. The optimum aged condition is then associated with cross-slip deformation. The fracture behavior of the overaged condition is a dynamic balance between a brittle matrix and the ductile (crack blunting) reverted austenite.

ALTHOUGH maraging steels have been commercially available for almost ten years, the factors controlling their fracture toughness are still unknown.[1] Previous investigations of the strength and fracture behavior of 18 pct nickel steels have been devoted to the 8 pct cobalt-type with strengths up to 300 ksi.[2,3] Recently, a 12 pct cobalt grade has been developed which can be heat treated to the 350 ksi strength level.[4,5] However, aircraft structural applications of this higher strength grade have been limited because of its low fracture toughness; the critical crack depth is approximately five times smaller than that for the most commonly used landing gear material (a silicon modified 4340).[5] This paper examines the fracture behavior in 18 Ni (350 ksi) maraging steel in various aged conditions and relates the strengthening mechanisms to the corresponding fracture toughness.

EXPERIMENTAL PROCEDURES

Two heats of consumable-electrode, vacuum remelted steel were obtained in the form of mill processed and annealed plate (products of Vasco Metals Inc., a Teledyne Company). The differences in form and chemical composition of each heat, as given in Table I, were minor so that no further differentiation between the heats is made in the presentation of results.

Standard Charpy impact specimens were prepared from both the longitudinal and transverse directions; the V-notch always lying in the rolling plane. The energy necessary for crack propagation was examined using fatigue precracked full size Charpy specimens.

Notched and smooth bar tensile specimens (0.25 in. diam) were machined from the longitudinal direction. Tensile tests were performed on either a 10,000 lb capacity Instron, 150,000 lb capacity Baldwin, or a 50,000 lb MTS High Rate Testing Facility, depending upon the strain rate of interest. The correlation between results obtained on different machines was excellent.

Table I. Chemical Composition of 18 Ni (350) Maraging Steel

Form	Material Composition							
	Ni	Co	Mo	Ti	Al	C	S	P
0.5 in. plate	18.3	11.9	4.72	1.42	0.13	0.007	0.005	0.002
0.625 in plate	18.51	11.89	4.67	1.53	0.09	0.008	0.006	0.003

Si	Mn	N	O	B	Zr	Ca
0.01	0.01	16 ppm	12 ppm	0.001	0.010	0.05
0.02	0.02	16 ppm	12 ppm	0.003	0.010	0.05

The amount of reverted or retained austenite was measured by the usual X-ray diffraction method of comparing integrated intensities.[6] Since the precipitation reactions involving molybdenum and titanium had progressed to a large extent prior to austenite formation, the austenite and martensite integrated intensities were compared assuming the two phases had identical composition. In addition, no corrections were made for the fact that a third phase was present, *i.e.*, the precipitates. These simplifying assumptions may result in a minor overestimation of the amount of reverted austenite.[7]

The influence of preferred orientation on austenite determination was examined by comparing the results of the direct $(200)_\alpha$—$(200)_\gamma$ comparison with a similar determination utilizing the $(211)_\alpha$—$(220)_\gamma$ peaks. Excellent agreement between these two comparisons was found. For example, after aging for 24 hr at 1100°F; 31.2 pct austenite was found using the $(200)_\alpha$—$(200)_\gamma$ combination while 30.9 pct austenite was found using the $(211)_\alpha$—$(220)_\gamma$ peak combination.

Samples for transmission electron microscopy were hand ground to 0.001 in. and thinned in a jet-polishing

H. J. RACK and DAVID KALISH are Scientists, Lockheed-Georgia Company, Marietta, Ga. This paper was presented at the 1970 TMS Fall Meeting in Cleveland, Ohio.

Manuscript submitted March 24, 1971.

Table II. Transformation Characteristics of 18 Ni (350) Marage Steel

Phase Transition	Temperature, °F
A_s (Austenite Start)	946 ± 5
A_f (Austenite Finish)	1430 ± 5
M_s (Martensite Start)	323 ± 5
M_f (Martensite Finish)	158 ± 5

apparatus using a chrome-acetic acid electrolyte.[8] After perforation and washing in dilute acetic acid and ethyl alcohol, the foils were dried and immediately examined in a JEM-7 microscope operated at 100 kv.

Crystallographic identification of the precipitate phases present was facilitated by using a calibrated (EFFA) measuring device for electron-diffraction patterns and comparing the results with those from anticipated precipitate phases. The lattice spacings and angles between planes for the anticipated non-cubic phases were generated using a computer program previously developed by Chilton and Barton.[9]

Finally neutron diffraction experiments were conducted to search for short and long range order. A description of the experimental procedures used in the neutron diffraction work is given elsewhere.[10]

EXPERIMENTAL RESULTS

Maraging Reaction

The continuous transformation characteristics (determined with a Leitz dilatometer) are given in Table II. The complete transformation to martensite after austenizing at 1500°F and air cooling to room temperature was confirmed by X-ray diffraction measurements.

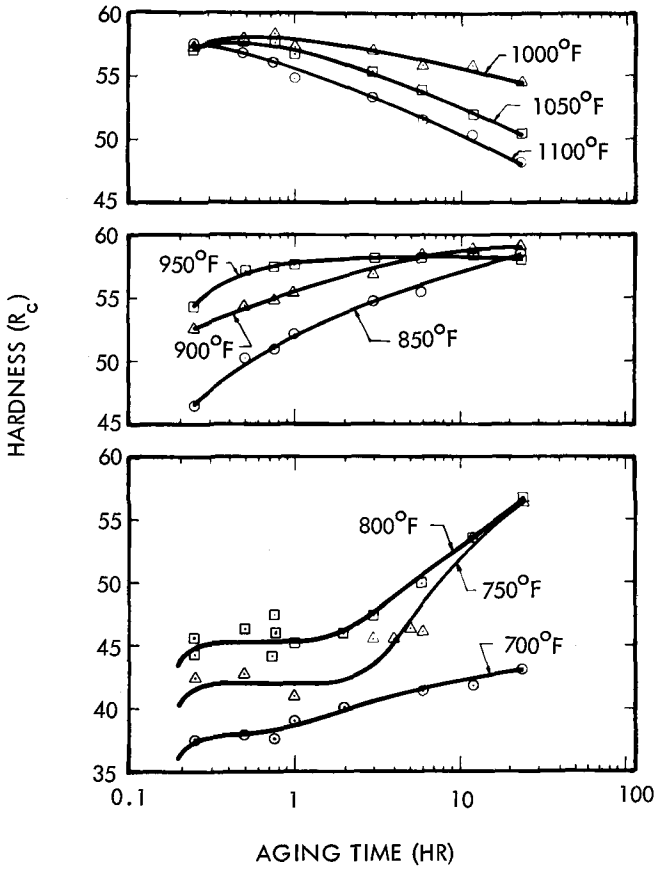

Fig. 1—Influence of aging time on hardness of 18 Ni (350) maraging steel.

The hardness of 18 Ni (350) maraging steel, upon aging at temperatures between 700° to 1100°F, is shown in Fig. 1. The aging response appears to fall into three distinct temperature regimes. Aging between 700° to 800°F results in a well defined hardness plateau. Aging at 850° to 950°F gives a continuous increase in hardness with aging time up to the maximum; slight overaging occurs within 24 hr at 950°F. Overaging occurs at 1000° to 1100°F within short times.

Fig. 2 shows that, during the aging times and temperatures considered in the present context, austenite is being formed. Notably, the initial formation of reverted austenite is associated with a slight overaging of the martensitic matrix.

Mechanical Properties

Tensile and fracture toughness were determined for selected heat treatments typical of three aging behaviors depicted in Fig. 2. The tensile properties are summarized in Table III. Neither underaging (800°F for 3 hr) or overaging (1100°F for 3 hr) results in an increase in the ductility relative to the optimum strength condition (950°F for 3 hr). The elongation, reduction of area, and notch tensile strength ratio all go through a maximum upon aging at 950°F for 3 hr. The ratio of the notched to unnotched tensile strength never exceeds unity in contrast to the behavior of lower strength maraging steels.[11]

The low ductility of underaged specimens is not associated with the plateau in hardness, Fig. 2. Indeed, as the aging time at 800°F increases, the strength increases and ductility decreases in a continuous manner, Fig. 3. The underaged alloy is very strain rate sensitive; as the strain rate increases the strength increases and the ductility increases, Fig. 4.

As illustrated previously for the tensile ductility, neither under- nor overaging results in any beneficial increase in the fracture toughness above that resulting from the optimum heat treatment, Table IV. Furthermore, underaging (800°F for 3 hr) produces a structure that is less resistant to rapid crack propagation as reflected by the precracked impact energy, than either optimum or overaging.

In the solutionized condition, the fracture toughness of this material is highly sensitive to specimen orientation, Table V. However, after aging, no anisotropy in toughness is observed. Evidently, without aging the austenite grain or inclusion structure must predominate, while after aging the precipitate structure must be most important.

If reverted austenite controls the fracture toughness we might expect a correlation between impact energy and the amount of reverted austenite, *e.g.*, upon aging at 1100°F. However, the fracture toughness is essentially independent of the volume percent reverted austenite, Fig. 5.

Microstructures

The austenitized and air cooled structure is a precipitate free martensite with a high dislocation density

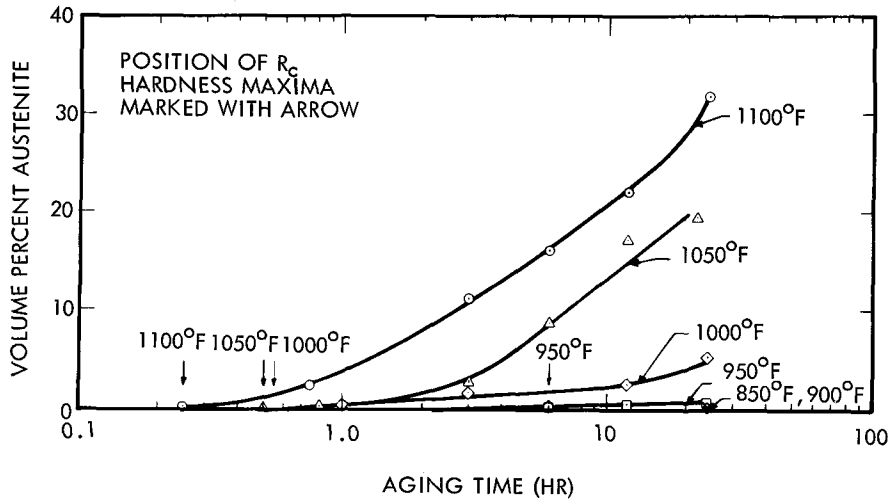

Fig. 2—Influence of aging time on volume per cent reverted austenite in 18 Ni (350) marag ing steel.

Table III. Tensile Properties of 18 Ni (350) Maraging Steel*

Condition	0.2 Pct YS, ksi	UTS, ksi	Elong., Pct	Red. Area, Pct	NTS/UTS, (K_t = 7.5)
1500°F (1 hr, AC)	123	157.1	19.1	73.7	0.9†
1500°F (1 hr, AC) + 800°F (3 hr, AC)	249.2	263.7	2.4	9.5	0.37
1500°F (1 hr, AC) + 950°F (3 hr, AC)	331.2	345.2	8.9	37.2	0.58
1500°F (1 hr, AC) + 1100°F (3 hrs, AC)	267.1	290.6	9.3	27.8	0.56

*Strain rate = 4.9 X 10^{-4}/sec = 2.9 X 10^{-2}/min.
†Gross yielding observed.

substructure, Fig. 6. Occasional microtwins were observed. The particles shown in Fig. 6, and found in other foils, are Ti(C, N) (~0.5 μ and spherical) and τ-Ti_2S (~1 to 5 μ and block-like); these undissolved inclusions are randomly dispersed throughout the matrix.

Some dislocation rearrangement associated with a deterioration of the martensite lath subboundaries occurs upon aging at 800°F.

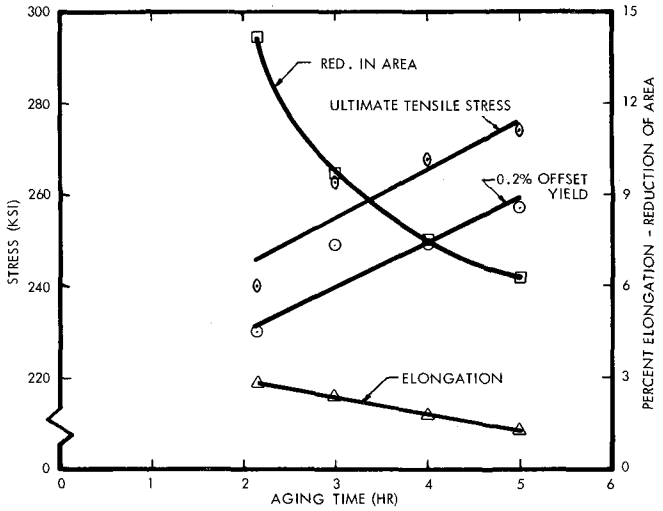

Fig. 3—Influence of aging time on mechanical properties of 18 Ni (350) maraging steel aged at 800°F.

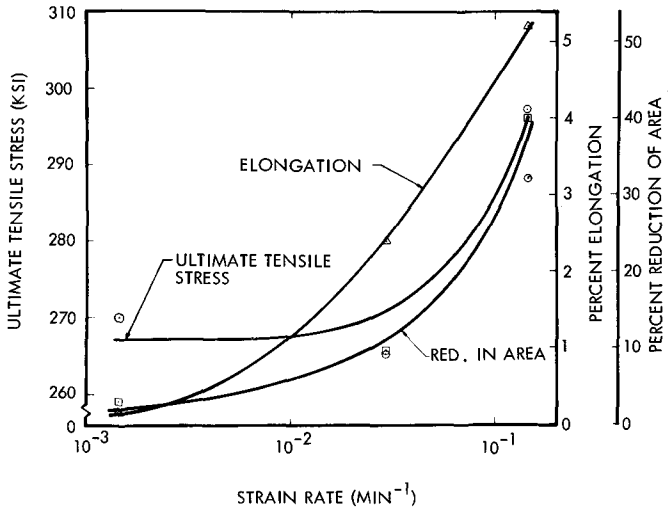

Fig. 4—Influence of strain rate on mechanical properites of 18 Ni (350) maraging steel aged for 3 hr at 800°F.

After aging for 3 hr at 800°F, there were still no precipitates [other than the Ti(C,N) and τ-Ti_2S particles] that could be extracted using standard extraction-replication techniques. However, an extremely fine precipitate was observed in the transmission specimens, Fig. 7. Selected area diffraction identified this fine spherical precipitate as a bcc structure similar to that observed by Abson and Whiteman[12] in an Fe-20Co-15Ni-8Mo alloy.

Table IV. The Influence of Heat Treatment on Fracture Toughness of 18 Ni (350) Maraging Steel

Condition	Impact Energy: Full Size, in.-lb/in.^{2}	Impact Energy: Precrack in.-lb/in.^{2}	Ratio: Precrack Energy To Full Energy
1500°F (1 hr, AC)	5690	3754	0.66
1500°F (1 hr, AC) + 800°F (3 hr, AC)	824	85	0.103
1500°F (1 hr, AC) + 950°F (3 hr, AC)	715	132	0.185
1500°F (1 hr, AC) + 1100°F (3 hr, AC)	706	134	0.19

Table V. Anisotropy of Fracture Toughness After Conventional Heat Treatment

Condition	Impact Energy, ft, lbs	
	Transverse	Longitudinal
1500°F (1 hr, AC)	58.79	105.7
1500°F (1 hr, AC) + 800°F (3 hr, AC)	8.55	9.08
1500°F (1 hr, AC) + 950°F (3 hr, AC)	7.36	7.5
1500°F (1 hr, AC) + 1100°F (3 hr, AC)	7.31	8.14

Aging for 3 hr at 950°F develops two clearly defined precipitate morphologies: rod-shaped orthorhombic Ni_3Mo and a spherical-shaped tetragonal σ-FeTi, Fig. 8. The Ni_3Mo precipitates tend to be larger than the σ-FeTi precipitates. In fact, only Ni_3Mo could be definitively identified using carbon extraction replicas (be-

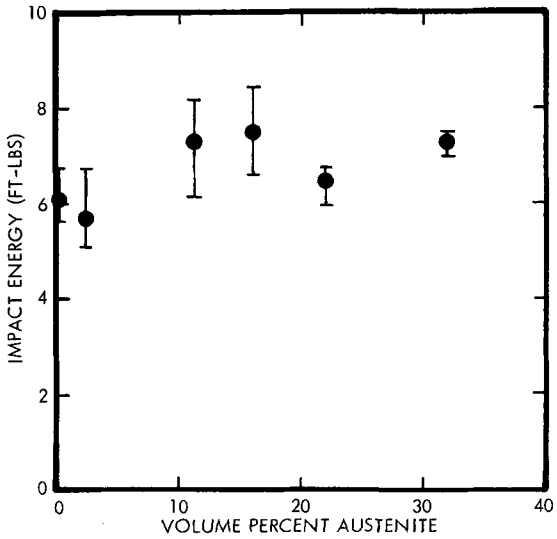

Fig. 5—Influence of amount of reverted austenite on fracture toughness upon aging at 1100°F.

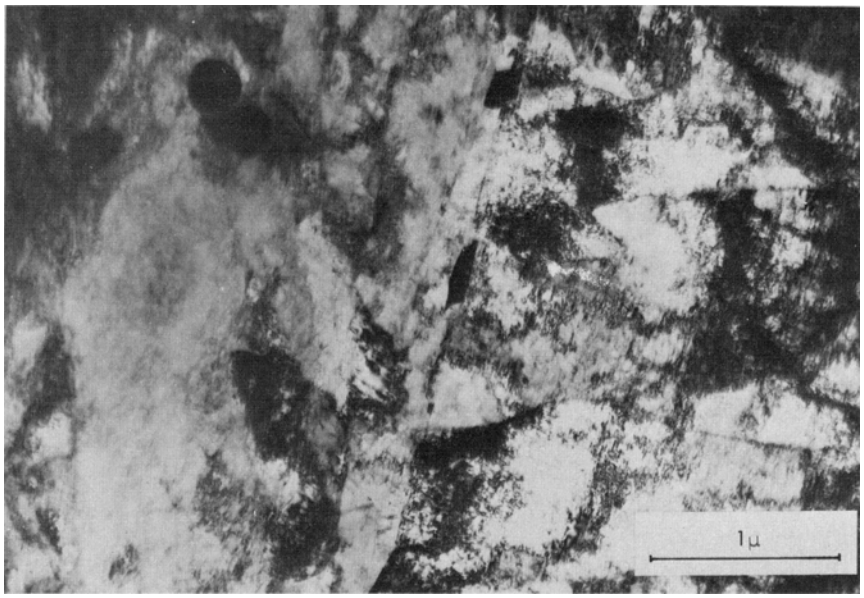

Fig. 6—Transmission electron micrograph of unaged 18 Ni (350) maraging steel (1500°F for 1 hr-AC).

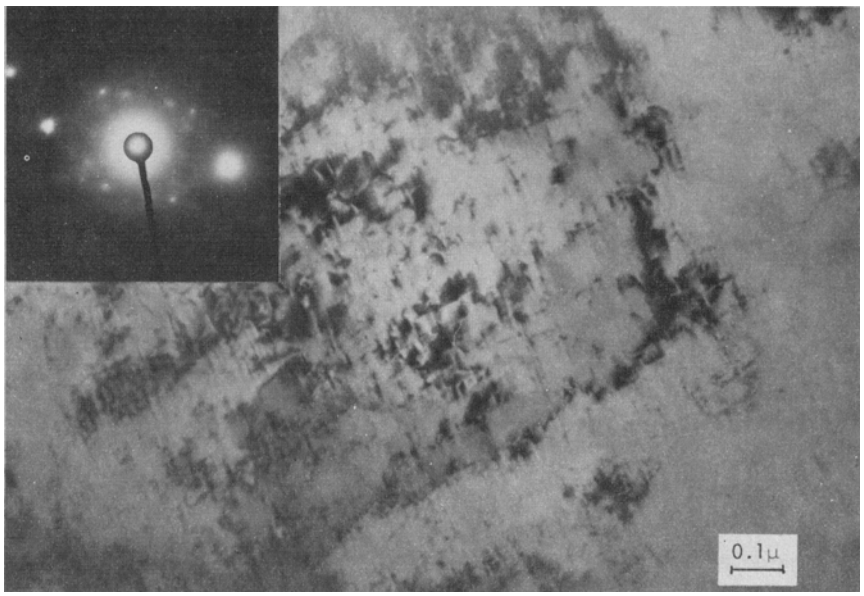

Fig. 7—Transmission electron micrographs of 18 Ni (350) maraging steel aged 3 hr at 800°F.

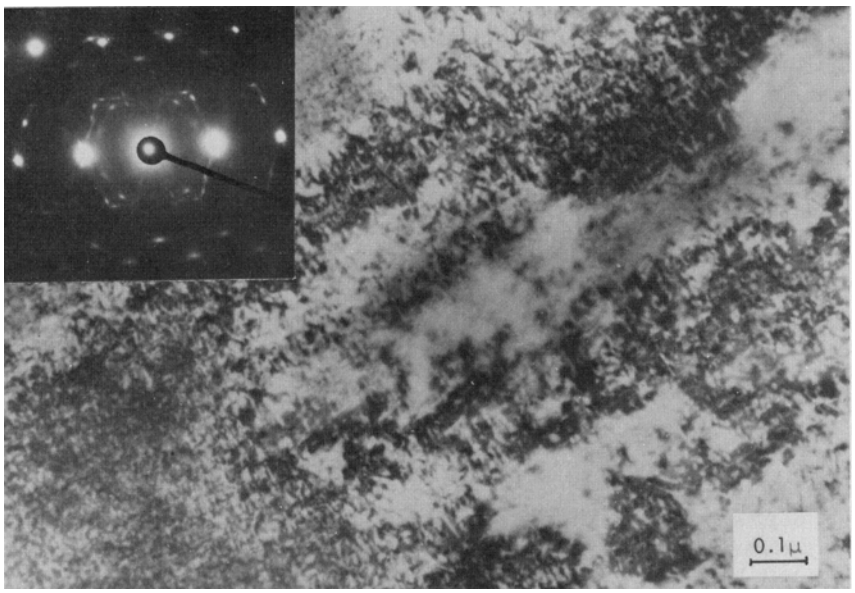

Fig. 8—Transmission electron micrographs of 18 Ni (350) maraging steel aged 3 hr at 950°F.

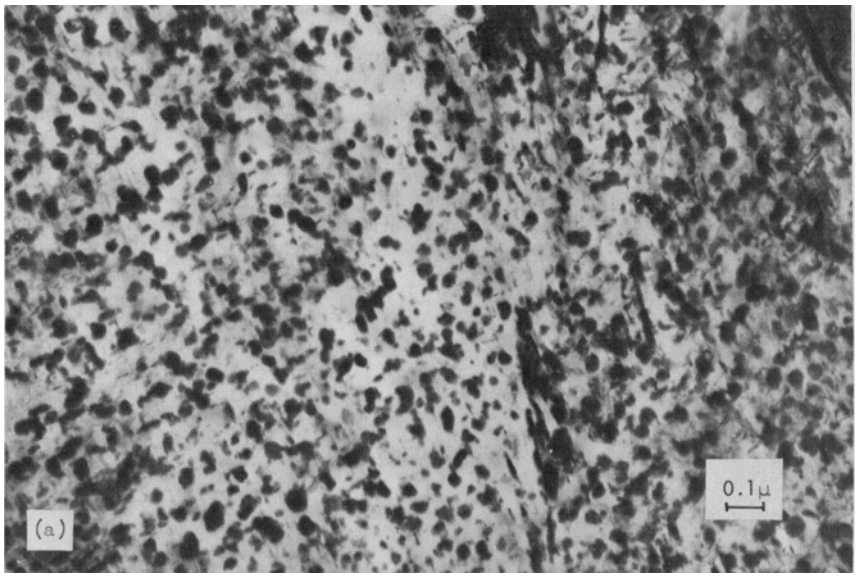

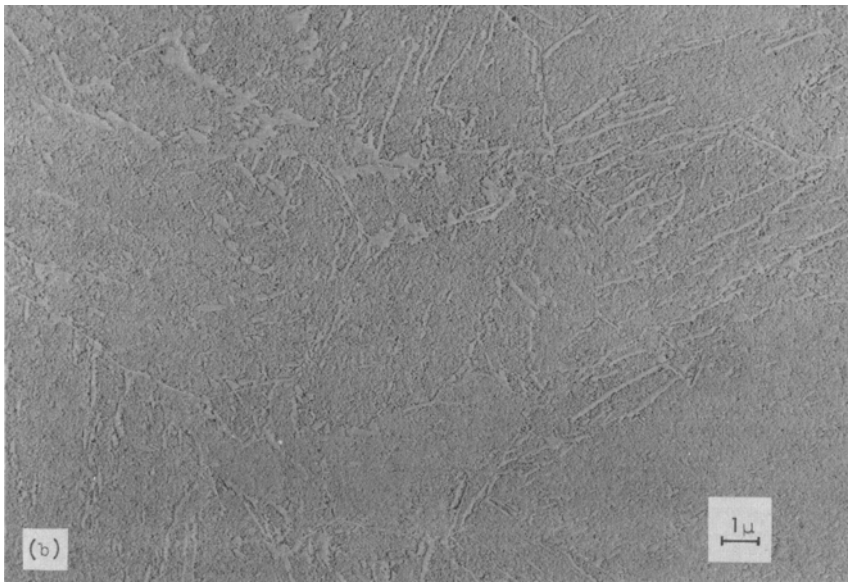

Fig. 9—Transmission (*a*) and replica (*b*) electron micrographs of 18 Ni (350) maraging steel aged 3 hr at 1100°F.

cause of difficulty encountered in extracting the smaller σ-FeTi precipitate). The precipitate sizes observed in the 18 Ni (350) maraging steel were compared to those in an 18 Ni (300) maraging steel,[3] the former being much finer. This is attributed, in part, to the influence of increased cobalt content. In addition, the volume fraction of σ-FeTi is higher, in the present case, as expected from the difference in titanium content, *i.e.*, 0.8 wt pct Ti in the 300 ksi grade and 1.5 pct Ti in the 350 ksi grade.

Substantial recovery of the dislocation substructure occurs during aging at 950°F and some evidence for grain or subboundary precipitation was observed. This is probably associated with the initial formation of reverted austenite; approximately 0.5 pct reverted austenite is present in this heat treatment condition, Fig. 2.

Overaging is characterized by a) an almost complete absence of a dislocation substructure, Fig. 9(*a*), and b) the presence of 12 vol pct reverted austenite located primarily at prior grain boundaries but also at martensite lath boundaries, Fig. 9(*b*). The precipitate substructure observed has coarsened with the Ni_3Mo phase having developed into large ellipsoids and the σ-FeTi precipitates into smaller rods, Fig. 9(*a*). Furthermore, small spheres, identified by selected area diffraction as Fe_2Mo, were occasionally observed.

Ordering of Cobalt

Neutron diffraction experiments, described in detail elsewhere,[10] established that no long range ordering of the cobalt occurs during aging of 18 Ni (350) maraging steel. However, distinct short range ordering of cobalt does occur. Since only the first diffuse scattering maxima was measured, no quantitative determination of the ordering coefficient was possible. Nevertheless, a comparison of calculated diffuse scattering profiles with calibrated data suggests that a) cobalt orders in the solid solution during aging, b) short-range ordering goes beyond first neighbors, and c) the first neighbor correlation parameter, α_1, is larger than the value allowed by uniform ordering.

Electron Fractography

The various precipitates have a marked influence on the fracture process. Fracture in the as-solutionized condition is transgranular with a non-uniform dimpled surface presumably due to the ductile nucleation, growth and coalescence of microvoids, Fig. 10. The larger dimples are associated with bulk particles, probably τ-Ti_2S or Ti(C, N), while the smaller dimples had a dispersoid free structure.

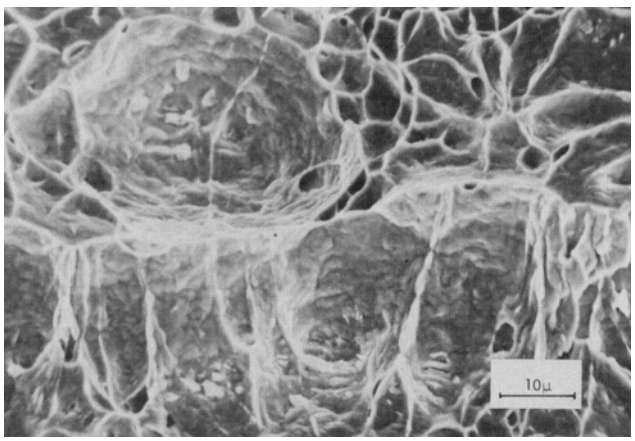

Fig. 10—Scanning electron micrograph of unaged 18 Ni (350) maraging steel.

Aging at 800°F also results in a predominantly ductile overstress fracture morphology, but with much smaller and uniform dimples than in the as-solutionized condition. However, the fracture appearance after tensile loading is dependent upon the strain rate and aging time. Decreasing the strain rate or the aging time at 800°F promotes increasing amounts of intergranular failure, Fig. 11. These intergranular regions are located at the periphery of the tensile specimen. Carter[5] has attributed this type of intergranular failure to an environmental effect on fracture and the strain rate effects reported herein substantiate this idea.

This intergranular fracture should not be confused with that due to grain boundary precipitates, as in the thermal embrittlement process.[13] The latter is established during hot working and annealing of the austenite and the entire fracture is intergranular. In this case, the alloy is not thermally embrittled and only the initial fracture is intergranular.

Increasing the strain rate also resulted in the formation of intergranular cracks parallel to the tensile loading direction, Fig. 12. These cracks may be a manifestation of increased ductility. If a propagating crack is locally deflected into a plane parallel to the major stress axis, it may be effectively blunted and an increase in stress will then be required to re-initiate another crack normal to the tensile axis before failure can be complete.

Fracture after aging for 3 hr at 950°F also occurred by coalescence of microvoids, Fig. 13. The dimple sizes associated with this process are slightly larger and less uniform than after aging at 800°F. The larger of these dimples could be associated with bulky particles, τ-Ti_2S or Ti(C, N) while the smaller dimples were essentially dispersoid free. Finally, evidence of reverted austenite fracture was observed at prior austenitic grain boundaries, in agreement with transmission electron microscopy which indicated reverted austenite formed at prior austenite grain boundaries with this aging temperature.

The substantial quantity of reverted austenite and the coarse precipitates that form upon aging at 1100°F for 3 hr produces a mixture of an extremely fine dimple rupture and quasi-cleavage, respectively, Fig. 14. The general fracture appearance is shown in Fig. 14(*a*) and the reverted austenite as compared to the aged martensite matrix is shown in Figs. 14(*b*) and 14(*c*). Although the reverted austenite may tend to increase the fracture resistance, the brittle behavior of the matrix counteracts this increase and there is no beneficial effect on toughness of overaging, in agreement with the fracture energy measurements.

DISCUSSION OF RESULTS

Maraging Reactions

The results of the present study suggest that the maraging reaction may be considered as a sequence of

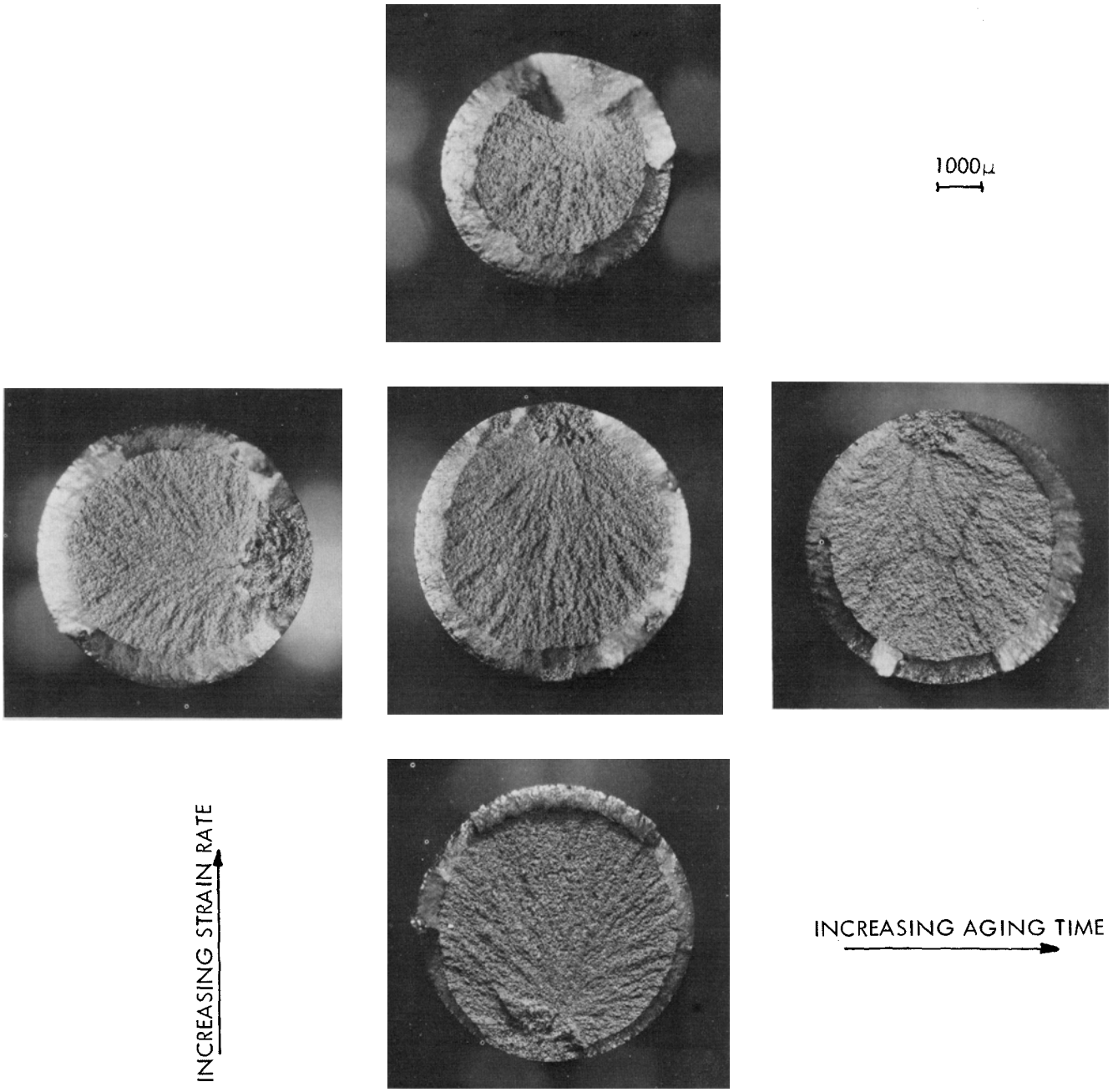

Fig. 11—Influence of strain rate and aging time on the fracture morphology of 18 Ni (350) maraging steel aged at 800°F.

quite simple steps. During the initial stage of age hardening, molybdenum atoms tend to cluster or form pre-precipitates and the cobalt assumes short range ordered positions. The rejection of nickel from the ordered Fe-Co regions and the clustering of molybdenum leads to the formation of Ni_3Mo. The nickel-lean (Co-Fe rich) regions serve as effective sites for σ-FeTi formation. Thus the presence of cobalt, in a short range order configuration, principally alters the size and extent of subsequent Ni_3Mo precipitation by altering the local solid solubility of molybdenum through the formation of nickel rich regions.

Ultimately the metastable Ni_3Mo and σ-FeTi precipitates coarsen and redissolve. This may lead to local enrichment of nickel at preferred sites, such as prior austenite or martensite plate boundaries, thus promoting the formation of equilibrium austenite.

This maraging sequence is also compatible with earlier investigations of lower strength maraging steels.[1] In the present instance the increased cobalt content, 12 pct as compared to 8 pct in 18 Ni (250) maraging steel, has made it possible to experimentally establish the role of this important alloying element.[10] It is now clear why the combined hardening effect of molybdenum and cobalt is much greater than that anticipated from their individual effects. Furthermore, it is apparent that the dislocation substructure is of secondary importance in describing the maraging reaction sequence. Peters and Floreen[14] arrived at a similar conclusion for the strengthening of an Fe-8Ni-13Mo alloy.

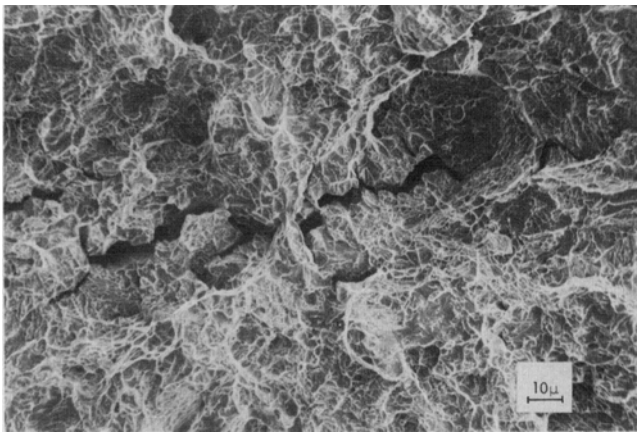

Fig. 12—Formation of secondary cracks in 18 Ni (350) maraging steel aged 3 hr at 800°F.

Strengthening and Fracture Mechanisms

The increase in strength observed from 18 Ni (250) to 18 Ni (300), and finally to 18 Ni (350) maraging steel is associated with the increasing titanium content which leads to an increase in the amount of σ-FeTi precipitation. The increased cobalt content of the 350 ksi alloy probably also decreases the size and spacing of the metastable Ni_3Mo.

The strengthening mechanism usually proposed as being responsible for the high strength in maraging steel has been the Orowan mechanism of dislocation bowing between precipitate particles. However, this mechanism cannot fully explain the behavior when Ni_3Mo is the principal precipitate.[1] Experimental verification of the Orowan mechanism has involved overaged structures[15,16] which are not representative of the optimum aging condition. Moreover, the cause of the high fracture toughness of 18 Ni maraging steels has not been apparent.

Floreen[1] has suggested that the high toughness associated with maraging steels may be due to the formation of a reverted austenite layer about the Ni_3Mo thus preventing void formation at the precipitates and thereby delaying ductile fracture. However, these layers have not been observed in this nor previous investigations.[2,3,9]

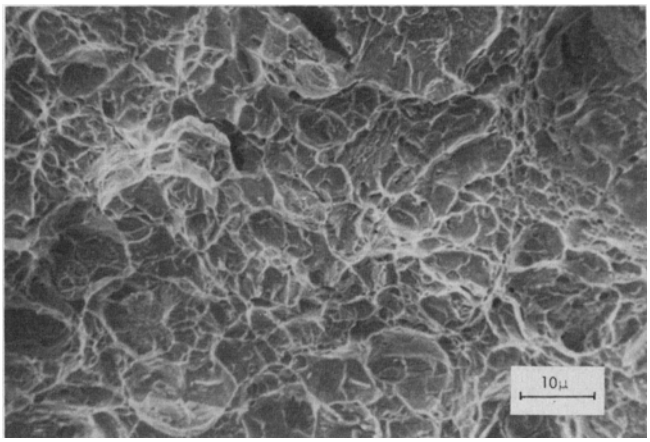

Fig. 13—Scanning electron fractograph of 18 Ni (350) maraging steel aged 3 hr at 950°F.

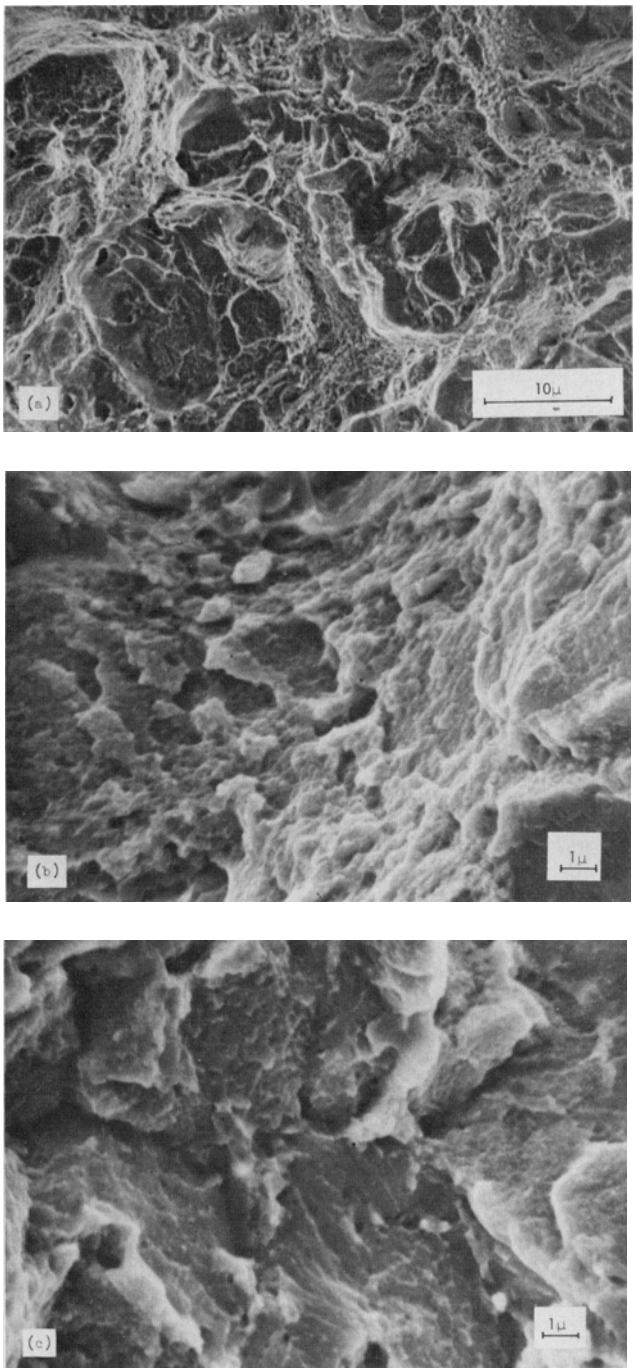

Fig. 14—Scanning electron fractographs of 18 Ni (350) maraging steel aged 3 hr at 1100°F.

The deformation characteristics of age-hardening systems may be examined in terms of the elementary dislocation-precipitate interactions involved. The formation of clusters (or coherent precipitates) in aluminum has been found to restrict cross-slip.[17] This coplanar slip mode increases the susceptibility of the material to stress corrosion cracking. The anomalous strain rate effects observed after aging 18 Ni (350) maraging steel for 3 hr at 800°F, where higher ductilities at higher strain rates are observed, can be attributed to an increased susceptibility to environment assisted cracking accompanying a planar slip mode.

During subsequent aging it will eventually become more energetically favorable for dislocations to leave the primary slip plane and thus bypass the precipitate particles than to cut them. The present instance is an extremely complicated matter since more than one type of precipitate, Ni_3Mo and σ-FeTi, is present and these particles not only possess long-range stress fields but also lead to short-range interactions. These interactions result from a) the development of long-range order within the particles,[18] and b) the "parelastic interaction" between the metastable particles and dislocations.[19,20] It is these interactions (in particular those arising from the metastable character of the precipitate substructure) that lead to the unique behavior observed in maraging steels with Ni_3Mo as their principal hardening agent.

Gerold and Haberkorn[21] have noted that the applicability of the cutting vs the bypass mechanisms depends, all other things being equal, on the ratio of the particle radius, R, to the Burgers vector, b. For $R/b \lesssim 15$, the cutting process is expected while for $R/b \lesssim 25$, the bypass mechanism is anticipated. In the present instance, aging at 800°F (3 hr) results in a precipitate substructure consistent with the cutting mechanism while aging at 950°F (3 hr) agrees with the bypass mechanism.*

*Precipitate particle diameters produced by aging at 800°F (3 hr) or 950°F (3 hr) were ~30Å and ~100Å, respectively.

Thus the high strength, high toughness characteristics of 18 Ni maraging steels may be attributed to the fine dispersion of the Ni_3Mo precipitates which, although offering a high resistance to initial dislocation motion, is of such a *size* and *spacing* that when dislocation motion does occur it occurs homogeneously throughout the microstructure. Although Ni_3Mo appears to be unique in this regard it is quite possible that the principal requirements of fine size and spacing may be achieveable by using other metastable precipitates. However, the attainment of this end requires a delicate balance between precipitate growth and coalescence and is beyond the scope of this paper.

Overaging in maraging steel is not a simple precipitate coarsening process. Rather, it is a duplex process involving the formation of a stable Fe_2Mo precipitate within the previous martensite matrix and of equilibrium reverted austenite. The deformation characteristics of the overaged matrix is similar to that observed in other overaged precipitation hardening systems. The primary strengthening mechanism is the bowing of dislocations between the large incoherent Fe_2Mo precipitate particles. The interparticle spacing is such (~400Å) that the matrix is weaker than that produced during optimum aging. Thus, the decrease in strength observed after aging at 1100°F (3 hr) is primarily due to the overaging of the matrix. This is in agreement with the recent investigation of Pampillo and Paxton.[22]

There is some evidence to indicate that reverted austenite may increase the uniform elongation[22,23] and perhaps the yield strength.[22] The reported beneficial influence of reverted austenite on the yield strength has been ascribed to added precipitation hardening by the reverted austenite at martensite lathe boundaries. In the present instance reverted austenite was primarily formed at prior austenite grain boundaries and is not thought to increase the yield strength above that of the overaged matrix.

Furthermore, from this study and others[5,22] it is clear that reverted austenite does not give a net increase in the fracture toughness above that of the peak-hardness condition. Perhaps, if the reverted austenite were not present, then overaging would result in a net decrease in the fracture toughness because the overaged particles serve as excellent crack nucleation sites. The crack blunting (or stress-relieving capability) of the reverted austenite prevents the fracture toughness from being even lower in the overaged condition, but no practical benefit from reverted austenite is offered.

The importance of dislocation-precipitate processes on the fracture toughness may be analyzed as by Hahn and Rosenfield.[24] The plane strain fracture toughness, K_{Ic}, depends upon the critical true strain at fracture, $\bar{\epsilon}^*$, the yield strength, Y, the Young's modulus E (assumed as a first approximation to be independent of heat treatment condition), and the strain hardening exponent, n, in the following manner.

$$K_{Ic} = [\tfrac{2}{3} EY\bar{\epsilon}^* (0.0005 + n^2)]^{1/2} \quad [1]$$

Although this expression may not give the exact plane strain fracture toughness parameter as measured directly under standardized test conditions, it is interesting to compare the ratio of K_{Ic} values calculated from Eq. [1] for aging at 800° and 950°F. This ratio, $K_{Ic}(800)/K_{Ic}(950) = 0.7$, Table VI,*† is in good agreement with the ratio of the square root of the precracked fracture energy, Table III, for these heat treatment conditions. At these high strength, low fracture toughness conditions, the precracked Charpy impact energy should be reasonably close to the plane strain critical extension force, G_{Ic}.*

*This analysis is valid only for failure modes that obey a strain critera. Since overaging produces a partial quasi-cleavage failure and thus does not obey such a criteria no direct comparison of the heat treatment condition with others can be made.

†See Table VI for a tabulation of the factors used.

*$K_{Ic}^2 = EG_{Ic} \approx E(W/A)$ if W/A pertains to a zero shear lip fracture, where W is the work required to fracture a precracked impact specimen and A is the area over which this work must be expended.[25]

The primary factor influencing the fracture toughness in this case is the critical true strain at fracture. Contrary to the expectations of Pampillo and Paxton,[22] the existence of a high strain hardening component is not sufficient reason to anticipate a high fracture toughness. Generally the critical true strain at fracture (in a strain criteria failure) is controlled by the ability of a material to respond plastically to a small increment in stress. If a small increment of stress cannot be accommodated by an accompanying increment in strain, crack or void initiation will occur. In addition, if the deformation behavior is constrained by the precipitate character, then the critical strain is controlled, on a microscale, by the ability of the dislocation substructure to respond to a further increase in stress. Since planar slip tends to confine subsequent deformation to highly localized regions, it is anticipated that structures exhibiting this deformation mode will not be as responsive to further increases in stress as those exhibiting a cross-slip deformation mode. In the latter case an increase in stress can be accommodated over a larger volume element due to the very nature of the associated slip process. Thus, the former aged condi-

Table VI. Numerical Parameters for Hahn-Rosenfield[24] Analysis

Aging Temperature	Y, ksi	$\bar{\epsilon}^*$ (a)	n	E, psi	Calculated, K_{Ic} Ksi $\sqrt{in}$	W/A(b) in-lb/in^2	$(EW/A)^{1/2}$ Ksi $\sqrt{in}$
800°F	249.2	0.099	0.059	27.0×10^6	42.1	85	48
950°F	331.2	0.467	0.030	27.0×10^6	62.3	132	59.9

(a) Assume $\bar{\epsilon}^* \cong ln$ (100/100–pct. reduction in area).
(b) Zero pct shear lip.

tion is expected to have a lower fracture toughness, as is observed. Finally then, in 18 Ni (350) maraging steel, it is the primary deformation mode that is the controlling factor in determining the fracture toughness.

ACKNOWLEDGMENTS

This work was performed in the Physical Metallurgy Team of the Materials Research Laboratory and was funded by the Lockheed-Georgia Co. Independent Research Program. The authors are indebted to J. W. Elling and K. D. Fike for their technical assistance in the experimental aspects of this investigation.

REFERENCES

1. S. Floreen: *Met. Rev.,* 1968, vol. 13, p. 115.
2. B. R. Banerjee, J. M. Capenos, and J. J. Hauser: *Advances in Electron Metallography,* p. 115, ASTM Spec. Tech. Pub. No. 396, 1966, Philadelphia, Pa.
3. W. A. Spitzig, J. M. Chilton, and C. J. Barton: *Trans. ASM,* 1968, vol. 61, p. 635.
4. G. W. Tuffnell and R. L. Cairns: *Trans. ASM,* 1968, vol. 61, p. 798.
5. C. S. Carter: *Met. Trans.,* 1970, vol. 1, p. 1551.
6. B. D. Cullity: *Elements of X-Ray Diffraction,* p. 391, Addison-Wesley Co., Inc., 1956, Reading, Mass.
7. D. T. Peters: *Trans. ASM,* 1968, vol. 61, p. 62.
8. R. D. Schoone and E. A. Fischione: *Rev. Sci. Inst.,* 1966, vol. 37, p. 1351.
9. J. M. Chilton and C. J. Barton: *Trans. ASM,* 1967, vol. 69, p. 528.
10. S. Spooner, H. J. Rack, and D. Kalish: *Met. Trans.,* 1971, vol. 2, p. 2306.
11. D. H. Yates and J. C. Hamaker: *Metal Progr.,* 1962, vol. 62, p. 97.
12. D. J. Abson and J. A. Whiteman: *J. Iron Steel Inst.,* 1970, vol. 208, p. 594.
13. D. Kalish and H. J. Rack: *Met. Trans.,* 1971, vol. 2, p. 2665.
14. D. T. Peters and S. Floreen: *Trans. TMS-AIME,* 1969, vol. 245, p. 2021.
15. B. G. Reisdorf and A. J. Baker: AFML-TR-64-390, 1965.
16. G. Pellester: *Problems in the Load-Carrying Application of High-Strength Steels,* p. 173, DMIC Rept. 210, 1964.
17. A. J. DeArdo, Jr. and R. D. Townsend: *Met. Trans.,* 1970, vol. 1, p. 2573.
18. S. Sato and P. A. Beck: *Trans. TMS-AIME,* 1959, vol. 215, p. 938.
19. H. Gleiter and E. Hornbogen: *Mater. Sci. Eng.,* 1967, vol. 2, p. 285.
20. E. Hornbogen and W. Meyer: *Acta Met.,* 1967, vol. 15, p. 584.
21. V. Gerold and H. Haberkorn: *Phys. Status Solidi,* 1966, vol. 16, p. 675.
22. C. A. Pampillo and H. W. Paxton: ONR Tech. Rept. Contr. Nonr. 760(14) NR 031-707, 1970.
23. P. Legendre: *Cobalt,* 1965, vol. 29, p. 171.
24. G. T. Hahn and A. R. Rosenfield: *Application Related Phenomena in Titanium Alloys,* p. 5, ASTM Spec. Tech. Pub. No. 432, 1968, Philadelphia, Pa.
25. B. S. Lement, K. Kreder, and H. Tushman: ASD-TDR-62-868, Part II, 1964.